Received: 9 July 2021 | Revised: 10 November 2021 | Accepted: 13 November 2021

DOI: 10.1111/gbb.12782

ORIGINAL ARTICLE

Genes, Brain and Behavior

MST1-knockdown protects against impairment of working memory via regulating neural activity in depression-like mice

Bin Chen | **Qiyue Zhang** | **Yuxing Yan** | **Tao Zhang**

College of Life Sciences and Key Laboratory of Bioactive Materials Ministry of Education, Nankai University, Tianjin, China

Correspondence
Tao Zhang, College of Life Sciences and Key Laboratory of Bioactive Materials Ministry of Education, Nankai University, 300071 Tianjin, China.
Email: zhangtao@nankai.edu.cn

Funding information
National Natural Science Foundation of China, Grant/Award Number: 32070988

Abstract

We reported that over-expression of MST1 induced the impairment of spatial memory via disturbing neural oscillation patterns in mice. Meanwhile, the P-MST1 is increased in the hippocampus after chronic unpredictable mild stress (CUMS). However, it is unclear if MST1 knockdown protects against stress-induced memory deficits via modulating neural activities. In the study, a CUMS mouse model was established and an intrahippocampal injection of AAV-shMST1 was used to knockdown MST1 in the hippocampus. The data showed that there were memory deficits with over-expressed P-MST1 level in CUMS mice. However, MST1 knockdown can significantly prevent the damages of CUMS-induced working memory and synaptic plasticity via regulating neural oscillation patterns. It suggests that MST1 down-regulation effectively protected against stress-induced behavioral dysfunctions. Moreover, as a more convenient way, neural oscillation analysis could provide some assistance for the auxiliary diagnosis and treatment of depression.

KEYWORDS
depression, hippocampus, knockdown, MST1, neural oscillations

1 | INTRODUCTION

The activated mammalian Ste20-like serine/threonine kinases 1 (MST1) was found in the central nervous system diseases, such as cerebral ischemia, stroke and amyotrophic lateral sclerosis (ALS),[1,2] which were related with cognition and memory. On the one hand, the abnormal MST1 level is related to neurological diseases. MST1 can phosphorylate FOXO protein, promote the transfer of FOXO to the nucleus, and induce nerve cell death,[3] while MST1 knockout alleviates the symptoms of ALS.[4] The phosphorylation levels of MST1 and Yap were significantly increased in Alzheimer's disease (AD)-like mice.[5] On the other hand, as a common and widespread psychiatric disorder, depression has been shown to damage cognition and memory.[6,7] Among them, a chronic stress-induced depression is a major category. Chronic stress for a long time can lead to working memory impairment and various mental diseases. One of the most classic depression models is the chronic unpredictable mild stress (CUMS) model. The continuous increase of glucocorticoid level, induced by chronic stress, impairs the induction of long-term potentiation (LTP).[8]

Neural oscillations are closely related to cognition in working memory tasks,[9] and could be a bridge between cognition and its molecular biological mechanism.[10] We know that different frequencies of neural oscillations are generally associated with different behaviors and cognition.[11] The analysis of neural oscillation can measure individual changes from the dynamic changes of brain network. One of our previous studies showed that over-expression of MST1 in the hippocampus disturbed the pattern of neural oscillation, and thereby impaired spatial memory in mice.[12] In addition, MST1

Bin Chen and Qiyue Zhang have contributed equally to this work

knockdown alleviated the CUMS-induced depression-like behavior.[13] However, the role of neural oscillations in the CUMS-induced working memory deficits is yet to be illuminated.

In the study, a hypothesis was raised that MST1 knockdown significantly protected against the impairment of working memory via modulating neural oscillation patterns in depression-like mice. This was done by establishing a mouse model of CUMS and a mouse model of MST1 knockdown by AAV. Working memory was measured and in vivo electrophysiological recordings were carried out. Both functional and structural synaptic plasticity were assessed. Finally, neural oscillation patterns were evaluated.

2 | MATERIAL AND METHODS

2.1 | Animals

C57BL/6N mice of 8 weeks old ($n = 30$, weight 25–30 g) were purchased from the Laboratory Animal Center of Academy of Military Medical Science of People's Liberation Army. The animals were reared under standard laboratory conditions (group-housed with 5 mice per cage; a constant temperature (22 ± 2°C); (lights on at 7 a.m.) a 12 h light/dark cycle) unless otherwise indicated. In addition, all animals allowed ad libitum access to food and water. All animal experiments were approved by the Animal Research Ethics Committee, Nankai University (20160004) and complied with the Animal Management Rules of the Ministry of Health of the People's Republic of China.

2.2 | AAV vectors injection

AAV 2/9 vectors for the MST1 knockdown (AAV-shMST1) and its control (AAV-shCtrl) were obtained from Hanbio Biotechnology (Shanghai, China). The titer of AAV is 1.0*10^11vg/ml. The shMST1 targeting sequence used GCCAGATTGTTGCAATCAAGC, and the control carried a scrambled shRNA. After 1 week of adaptation with the artificial environment, the animals were anesthetized with 10% chloral hydrate (4 ml/kg body weight, i.p.) and placed in the stereotaxic frame (SN-3, Narishige, Japan). After that, the infusions of AAVs into the bilateral hippocampus (anterior–posterior position −2.0 mm, medial-lateral position ±1.4 mm, 1.5 mm dorsoventral from the bregma) were performed at a flow rate of 0.5 μL/min (1 μL/side) using a 10-μL Hamilton syringe (Hamilton Co., Reno, NV). 10 min of rest was employed to allow diffusion after the injection.

2.3 | CUMS procedure

After AAV vectors injection for 7 days, the experimental mice were reared individually and exposed to different stressors over the course of 4 weeks. Briefly, the mild stress paradigm was as follows: Ice water swimming (4°C, 1 min), reversed light/dark cycle (24 h), oven (45°C, 5 min), cage tilt (45°, 12 h), damp bedding (150 ml water +200 g bedding, 24 h), tail pinch (1 min), white noise (85 dB, 5 min), confinement in tube (2 h), and water and food deprivation (24 h). These stressors were randomly scheduled during the modeling period.

Mice in the experiment were mainly divided into three groups. (1) the CON group: injected with AAV-shCtrl ($n = 7$); (2) the CUMS group: injected with AAV-shCtrl exposed with CUMS ($n = 7$); (3) the CUMS+MST1 group: injected with AAV-shMST1 exposed with CUMS ($n = 7$). In addition, the CON+MST1 group: injected with AAV-shMST1 only for Western blot assay ($n = 3$).

For the LPS-induced model, mice were randomly allocated to the CON group ($n = 3$) and LPS group ($n = 3$). Mice were intraperitoneally injected with normal saline in the CON group and the animals were intraperitoneally injected with 0.83 mg/kg LPS in the LPS group.

2.4 | Sucrose preference test

The sucrose preference test contains two paradigms, including a 3-day adaptation and a 2-h test. On the first day of adaptation, all mice were individually placed in cages with two identical bottles containing 1% sucrose solution. The next day we changed one of the two bottles to water, and exchanged the positions of the two bottles after 12 h to reduce any positional deviation. On the last day, the animals could not get food and water. During the 2 h of the test, the mice were free to choose two bottles containing 1% sucrose solution or water. We calculated the sucrose preference value following formula: sucrose preference (%) = sucrose intake (ml)/[sucrose intake (ml) + water intake (ml)] × 100%.

2.5 | Novel object recognition test

The experiment was carried out in the same place as the open field test. We let each mouse freely explore two identical objects A on the same side of the box for 5 min. After 2 h, replace one of the subjects A with a new subject B, and then let the animal explores the two subjects for 5 min. After 24 h, replace the new object B with another new object C, and allow to explore for another 5 min. Record the number of explorations of the old object and the novel one to calculate the recognition index by the following formula: $Number_{novel}/(Number_{novel} + Number_{old})$ *100%, to assay recognition memory ability.

2.6 | In vivo electrophysiological recording

Mice were placed in a stereotactic frame (Narishige, Japan) after anesthetized by urethane (1.2 g/kg body weight; i.p.). The scalp of mouse was incised and two small holes were drilled in the skull of the left side for electrode implantation, according to the mouse brain atlas. A bipolar stimulating electrode was slowly implanted into the perforant pathway (PP: anterior–posterior position 3.8 mm, medial–lateral position 3 mm, 1.5 mm dorsoventral from the bregma), another electrode

was positioned into the dentate gyrus (DG: 2.0 mm anterior to the bregma, 1.4 mm lateral to midline, 1.5 mm ventral below the dura). Correct placement was controlled by the electrophysiological criteria of this synaptic circuit, especially regarding electrode depth. The signals of local field potentials (LFPs) were acquired at a sampling rate of 1000 Hz for 15 min.

Afterwards, we measured the LTP and depotentiation (DEP) of the pathway. The field excitatory post-synaptic potentials (fEPSPs) of the hippocampal DG region were evoked by the stimulation of the PP, and the amplitude was used to assess the synaptic efficacy. Firstly, a stimulative optimal intensity that could evoke 70% response of its maximum amplitude (range 0.3–0.5 mA) was delivered at single-pulse stimulation to record a 20-min baseline (Scope software, PowerLab). After theta burst stimulation (TBS) including of 30 trains of 12 pulses (200 Hz) at 5 Hz, the LTP was recorded every 60 s for 1 h. After the LTP, low-frequency stimulation (LFS, 1 Hz, 15 min) was delivered to induce DEP. The fEPSPs of DEP were recorded for 1 h similarly. The evoked response of the last 20 min of LTP was normalized and used as the baseline of the DEP. The original analysis of all the data was conducted through Clampfit 10.2 (Molecular Devices, Sunnyvale, CA, USA).

2.7 | Total proteins extract and Western blot assay

After LFP recording, the animals were decapitated, and then the hippocampus was quickly removed and stored at −80°C. Hippocampal tissues were ground and lysed in 200 μL of lysis buffer (Beyotime Biotechnology, Haimen, China) which contained a protease inhibitor cocktail (1: 100 dilution). The homogenate was then centrifuged at 12,000 rpm at 4°C for 15 min, and the supernatant was collected. After that, the protein concentration was measured using BCA assay kit (Beyotime Biotechnology, Haimen, China), separated an equal amount of protein loaded by SDS-PAGE on a 10%–13% gels and transferred it to a PVDF membrane (Millipore, USA) by electrophoresis. The PVDF membranes were blocked in 10% skimmed milk for 1 h at RT and incubated overnight at 4°C with primary antibodies. On the second day, the PVDF membrane was washed 4 times with Tris-buffered saline containing 0.05% Tween 20 (TBST) and incubated the horseradish peroxidase-conjugated secondary antibody (1:4000 dilution; Promega, USA) for 2 h at RT, then washed again four times. After that, they were detected and analyzed using a computerized chemiluminescent imaging system (Tanon 5500, Tanon Science & Technology, China). Glyceraldehyde-3-phosphate dehydrogenase (GAPDH) was utilized as an internal control. A computerized chemiluminescent imaging system (Tanon 5500, Tanon Science & Technology, China) was used to define the protein band intensities. The NIH Image J program was used to quantify the bands. All the antibody we used were as following: anti-P-MST1 (1:2000, Abcam, UK), anti-MST1 (1:2000, Abcam, UK), anti-GAPDH (1:2000, Abcam, UK), anti-PSD95 (1:2000, Abcam, UK), anti-SYP (1:2000, Abcam, UK).

2.8 | Golgi staining

The Golgi–Cox staining procedure includes (1) the brain tissue is quickly removed from the skull and soak it in the Golgi staining solution at 4°C in the dark for 14 days. The Golgi staining solution needs to be replaced every 2 days; (2) The brain is sliced into 150-μm thick coronal sections by vibratome (Campden Instrument Ltd., MA752, England); (3) All slices are placed in 6% sodium carbonate solution (pH = 10.06) for 20 min, distilled water for 1 s, 70% alcohol for 10 min, 90% alcohol for 15 min, 100% alcohol for 20 min, and xylene for 20 min in proper order; (4) The slices are mounted on slides with DPX and cover glassed; (5) Then a light microscope (Magnus MLX) is used to evaluate the morphology and density of dendritic spines in the DG area. Only granular cells, whose soma and primary dendrites were clearly stained, were selected for analysis. The dendrites should be distinguished from those of neighboring cell bodies. To count the dendritic spines, straight branches that provided a clear resolution of spines and longer than 20 μm were preferred. We analyzed three mice in each group and selected three dendritic spines per mouse for statistical analysis ($n = 3$).

2.9 | Neural oscillatory analysis

After obtaining LFP data, offline analysis was performed. First, the original data were filtered at 0.5–100 Hz. Then, according to the need of later analysis, the frequency bands were divided into three bands, including theta (3–8 Hz), low gamma (LG, 30–50 Hz) and high gamma (HG, 50–100 Hz).

2.9.1 | Power spectra

Chronux routines were applied to calculate power spectrum.[14] The corresponding parameters are: sliding windows of 10 s with 50% overlap and the Slepian tapers field as (5–9). The power of each frequency band was then normalized by the sum power across bands (0.5–100 Hz) for the statistics.

2.9.2 | Phase locking value

Phase locking value (PLV) is an important synchronization index of the same rhythm, which focuses on evaluating the synchronization intensity of different neural oscillations. The specific steps of the algorithm are as follows, (1) raw LFP signals were filtered by EEGLAB toolbox (1 Hz bandwidth and 1 Hz step), (2) the Hilbert transform was applied to calculate and extract the instantaneous phases of filtered LFPs. In this study, a time window length of 10,000 (10 s) with 50% overlap was chosen. The range of PLV was 0–1, where 1 and 0 represented for full synchronization and no synchronization at all.

2.9.3 | Evolution map approach

Evolution map approach (EMA) is an algorithm proposed by Rosenblum and Pikovsky to measure the coupling direction and strength between two signals.[15] This is an analysis algorithm based on the theory of phase dynamics, which estimates the coupling direction by reconstructing the phase dynamics system. For a more detailed description to the algorithm, one can refer to our pervious article.[16] The directional index coefficient of the algorithm is expressed as *d* index. Suppose that the data of two channels are *X1* and *X2* respectively. When $d = 1$, it means that *X1* has influence on *X2*, and *X2* has no influence on *X1*. When $d = 0$, the influence of both sides is symmetric; when $d = -1$, it means that *X2* has complete influence on *X1*, and *X1* has no influence on *X2*.

2.9.4 | Phase-amplitude coupling

Phase amplitude coupling (PAC) is one of the most representative phenomena of cross-frequency coupling (CFC). The PLV algorithm is also widely used in cross-frequency coupling, which has good adaptability and only needs a little modification. Similarly, the low frequency phase and high frequency rhythm amplitude of the signal are extracted by Hilbert transform. Then, Hilbert transform is used again to get the phase of the extracted high frequency rhythm amplitude. Further, the PLV algorithm is used to calculate. In our study, we computed and analyzed PLV between theta and gamma oscillations. In the calculation program, 40 s of data length is used with 50% overlap. The values of PAC-PLV range from 0 to 1, where 1 means that the low and high frequency rhythms are completely synchronized, and vice versa.

2.10 | Data and statistical analysis

All data were statistically analyzed using SPSS 19.0 (SPSS Inc., Chicago, USA) and expressed as mean ± SEM. The Student's *t* test evaluates the statistical significance of the difference between the two groups. One-way ANOVA followed by Tukey HSD post hoc tests was employed to analyze the data obtained for the comparison of three groups (CON, CUMS and CUMS+MST1). When $p < 0.05$, the difference is considered to be statistically significant.

3 | RESULTS

3.1 | MST1 knockdown protected against CUMS-induced working memory impairment

A considerable amount of literature shows that chronic stress is closely related to depression.[17] CUMS is a reliable and effective rodent model of depression built on chronic stress.[18] A sucrose preference test was performed, and it was found that the sucrose preference was significantly decreased in the CUMS group compared to that in the CON group (Figure 1I $p = 0.000$; Three groups: F (2, 18) = 54.573, $p = 0.000$), suggesting that CUMS caused depression-like anhedonia. Western blotting data showed that there was no significant difference of the total MST1 expression between the CON group and the CUMS group (Figure 1B $p = 0.990$; Four groups: F (3, 8) = 7.491, $p = 0.010$), however, the level of P-MST1 (Figure 1C $p = 0.000$; Four groups: F (3, 8) = 223.040, $p = 0.000$) and the ratio of P-MST1/MST1 (Figure 1D $p = 0.034$; F (3, 8) = 8.525, $p = 0.007$) were significantly increased in the CUMS group compared to that in the CON group, implying that MST1 was phosphorylated in the CUMS group. Moreover, we further measured the same indicators in the model of LPS-induced depression. There was no significant difference of the total MST1 expression (Figure 1F: t (4) = −0.003, $p = 0.998$). The level of P-MST1 was higher in the LPS group than that in the CON group (Figure 1G: t (4) = −3.830, $p = 0.019$). The ratio of P-MST1/MST1 was significantly increased in the LPS group compared to that in the CON group (Figure 1H: t (4) = −3.312, $p = 0.030$). Clearly, the result was consistent with the CUMS-induced depression model.

Nevertheless, knockdown MST1 significantly improved the impairments induced by CUMS. The level of the total MST1 was lower in the CON+MST1 group than that in the CON group (Figure 1B $p = 0.036$), and was also lower in the CUMS+MST1 group than that in the CUMS group (Figure 1B $p = 0.047$). Furthermore, the level of P-MST1 was lower in the CUMS+MST1 group than that in the CUMS group (Figure 1C $p = 0.000$). In addition, knockdown MST1 did not significantly affect the P-MST1/MST1 ratio between the CUMS group and CUMS+MST1 group (Figure 1D $p = 0.054$).

It was found that the CUMS-induced decrease in sucrose preference was significantly improved in the CUMS+MST1 group (Figure 1I $p = 0.000$). In addition, the hippocampal-related working memory was tested by using the NOR test (Figure 1J). In the training stage, there is no statistical difference in the recognition index among these three groups (Figure 1K, F (2, 18) = 0.235, $p = 0.793$). In the 2 h and 24 h tests after training, the recognition index was lower in the CUMS group than that in the CON group (2 h: $p = 0.030$; 24 h: $p = 0.038$; 2-h report among three groups: F (2, 18) = 5.185, $p = 0.017$; 24-h report among three groups: F (2, 18) = 4.836, $p = 0.021$), however, it was significantly increased in the CUMS+MST1 group compared to the CUMS group (2 h: $p = 0.032$; 24 h: $p = 0.038$).

3.2 | MST1 knockdown prevented CUMS-induced synaptic plasticity damage

It is well known that synaptic plasticity is closely related to neural oscillations.[19] We performed in vivo electrophysiological tests to evaluate synaptic plasticity in the hippocampus, including LTP and DEP (Figure 2A–C). As soon as delivering TBS, the amplitude of fEPSPs was increased, and the amplitude was lower in the CUMS group than that in the CON group (Figure 2B $p = 0.000$; Three groups: F (2, 18) = 27.793, $p = 0.000$), but MST1 knockdown effectively

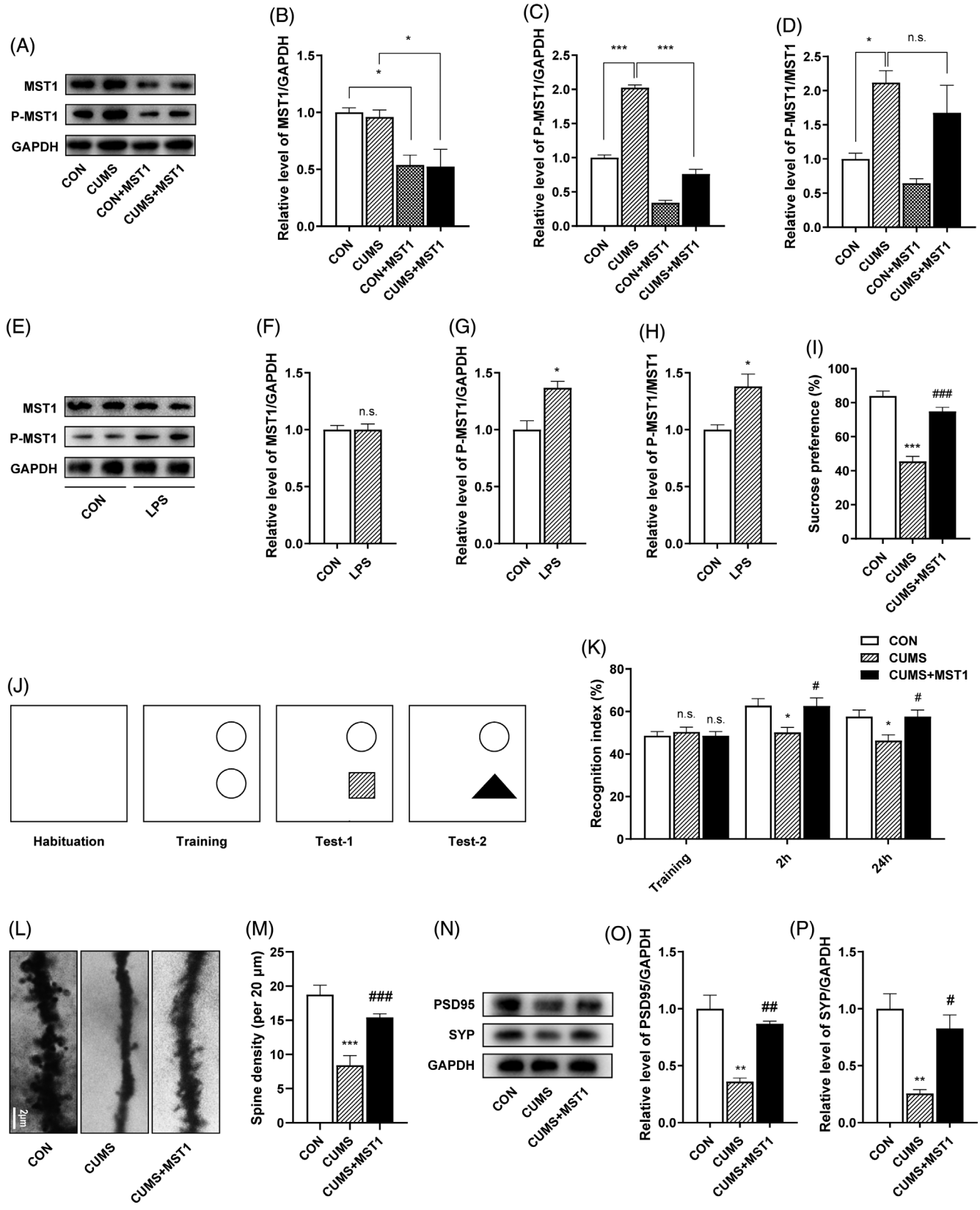

FIGURE 1 Legend on next page.

prevented LTP damage (Figure 2B $p = 0.000$). As we known that low-frequency stimulation (LFS) could induce DEP. The fEPSPs amplitude was higher in the CUMS group than that in the CON group (Figure 2C $p = 0.003$; Three groups: F (2, 18) = 7.940, $p = 0.003$), while MST1 knockdown significantly alleviated the DEP damage ($p = 0.020$). Dendritic spines are the functional protrusion of synapses, and their formation and elimination are manifestations of the synaptic structural plasticity. Therefore, we observed the tertiary dendritic profiles of granule cells from the DG region by using Golgi-Cox staining (Figure 1M). There are the quantitative statistical results of dendritic spine density among them (n = 3), as shown in Figure 1M (F (2, 6) = 61.206, $p = 0.000$; CON versus CUMS: $p = 0.000$; CUMS versus CUMS+MST1: $p = 0.001$).

To further evaluate synaptic integrity, we quantified the expression of the presynaptic vesicle membrane synaptophysin (SYP) and the postsynaptic density protein 95 (PSD95) in the hippocampus (Figure 1N–P, SYP among three groups: F (2, 6) = 13.898, $p = 0.006$; PSD95 among three groups: F (2, 6) = 21.486, $p = 0.002$). Western blot results showed that CUMS significantly decreased the level of these two pre- and post-synaptic proteins in the hippocampus (Figure 1O, PSD95: $p = 0.002$; Figure 1P, SYP: $p = 0.006$). However, these deficits were significantly mitigated in the CUMS+MST1 group compared to that in the CUMS group (Figure 1O, PSD95: $p = 0.006$; Figure 1P, SYP: $p = 0.019$).

3.3 | MST1 knockdown suppressed CUMS-induced power distributions disorder

Power spectrum is the most widely used index to measure the power intensity of signal. Figure 2D showed the normalized power distribution in the DG at 1–100 Hz. The power value at theta band was lower in the CUMS group than that in the CON group, while it was higher in the CUMS+MST1 group (Figure 2E, F (2, 18) = 23.917, $p = 0.000$; CON versus CUMS: $p = 0.000$; CUMS versus CUMS+MST1: $p = 0.000$). At the same time, the power value was relatively high in the CUMS group compared to that in the CON group at both LG and HG bands, while MST1 knockdown significantly reduced the value in CUMS-induced power (Figure 2F left, F (2, 18) = 3.901, $p = 0.039$; CUMS versus CUMS+MST1: $p = 0.035$; Figure 2F right, F (2, 18) = 3.738, $p = 0.044$; CUMS versus CUMS+MST1: $p = 0.043$). The similar data could be also obtained from the power spectrum analysis of PP signals (Figure S1A–C).

3.4 | MST1 knockdown protected against disturbance of neural information communication

It was found that the PLV at theta band was lower in the CUMS group than that in the CON group, while it was higher in the CUMS+MST1 group than that in the CUMS group (Figure 2G, H, F (2, 18) = 5.727, $p = 0.012$; CON versus CUMS: $p = 0.049$; CUMS versus CUMS +MST1: $p = 0.031$). As a directivity index, Figure 2I showed the value of EMA in the frequency range of 1–100 Hz. Moreover, EMA index from PP to DG at theta band was lower in the CUMS group than that in the CON group, while it was higher in the CUMS+MST1 group than that in the CUMS group (Figure 2J, F (2, 18) = 3.819, $p = 0.041$; CON versus CUMS: $p = 0.046$; CUMS versus CUMS+MST1: $p = 0.019$).

The PAC-PLV algorithm was used to measure theta-gamma cross-frequency coupling strength. Figure 2K showed a typical PAC between PP and DG in these three groups. The gamma band was further divided into low-gamma (LG) and high-gamma (HG). Figure 2L and Figure S1D shows the measurement of PAC. The theta-HG PAC between PP and DG was smaller in the CUMS group than that in the CON group, however, it was bigger in the CUMS + MST1 group than that in the CUMS group (Figure 2L right, F (2, 18) = 5.791, $p = 0.011$; CON versus CUMS: $p = 0.004$; CUMS versus CUMS+MST1: $p = 0.031$). Furthermore, The theta-HG PAC in the hippocampus DG was smaller in the CUMS group than that in the CON group, but it was higher in the CUMS + MST1 group than that in the CUMS group (Figure 2L middle, F (2, 18) = 3.83, $p = 0.041$; CON vs. CUMS: $p = 0.019$; CUMS vs. CUMS+MST1: $p = 0.044$;). We also measured the theta-LG PAC (Figure S1D).

FIGURE 1 (A) The representative immunoreactive bands of total MST1 and P-MST1 in the four groups. (B) The expression of MST1 was significantly reduced in the CON+MST1 group and the CUMS+MST1 group ($n = 3$). (C) Hippocampal MST1 knockdown could effectively prevent the CUMS-induced increase of P-MST1 ($n = 3$). (D) CUMS increased P-MST1/MST1 ratio ($n = 3$). (E) The representative immunoreactive bands of total MST1 and P-MST1 in the CON group and the LPS group. (F) There was no significant effect on the expression of MST1 in the LPS group ($n = 3$). (G) LPS increased the expression of P-MST1 ($n = 3$). (H) LPS increased the P-MST1/MST1 ratio ($n = 3$). (I) Hippocampal MST1 knockdown can effectively restore the reduced sucrose preference caused by CUMS ($n = 7$). (J) The experiment protocol of NOR test. (K) Hippocampal MST1 knockdown can effectively restore the reduced hippocampal-related recognition memory caused by CUMS ($n = 7$). (L) Representative images of dendritic spine in three groups. (Scale bar is 2 μm). (M) Hippocampal MST1 knockdown prevented the impairment of spine density induced by CUMS in Golgi staining ($n = 3$). (N) The representative immunoreactive bands of PSD95 and SYP in three groups. (O) Hippocampal MST1 knockdown can effectively restore the reduced the decrease in PSD95 expression caused by CUMS ($n = 3$). (P) Hippocampal MST1 knockdown can effectively restore the reduced the decrease in SYP expression caused by CUMS ($n = 3$). Data are expressed as mean ± SEM. $^{*}p < 0.05$, $^{**}p < 0.01$, $^{***}p < 0.001$ comparison between the CON group and CUMS group; #$p < 0.05$, ##$p < 0.01$, ###$p < 0.001$ comparison between the CUMS group and CUMS+MST1 group

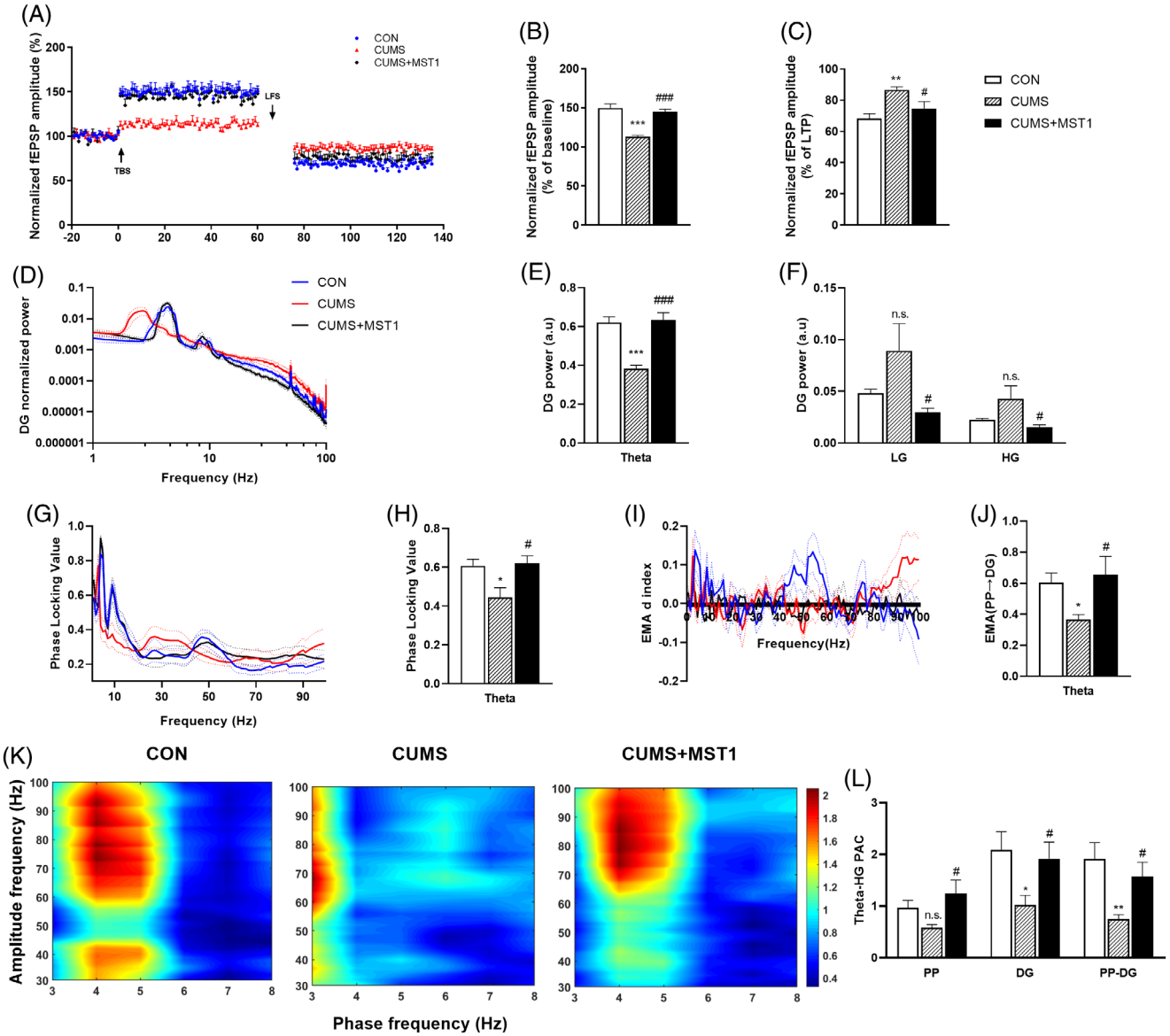

FIGURE 2 LTP, DEP, power spectrum, phase synchronization, directivity index of EMA and cross-frequency coupling analysis in PP and DG area. (A) The changes of time coursing in the fEPSPs amplitudes in both LTP and DEP stages in the three groups. (B) Hippocampal MST1 knockdown effectively alleviated the LTP damage induced by CUMS ($n = 7$). (C) Hippocampal MST1 knockdown significantly alleviated the DEP damage induced by CUMS ($n = 7$). (D) 1–100 Hz mean power spectrum in DG area. (E) The statistical result of power distribution at theta (3–8 Hz) in DG area. (F) The statistical results of power distribution at LG (30–50 Hz) and HG (50–100 Hz) in DG area. (G) The mean PLV in the range of 1–100 Hz. (H) The statistical result of PLV at theta (3–8 Hz). (I) The EMA index d from PP to DG. (J) The statistical result of EMA at theta (3–8 Hz). (K) The mean PAC between low frequency rhythm (3–8 Hz) and high frequency rhythm (30–100 Hz). (L) The statistical results of theta (4–5 Hz)-HG (50–100 Hz) PAC. Data are expressed as mean ± SEM. $^{*}p < 0.05$, $^{**}p < 0.01$, $^{***}p < 0.001$ comparison between the CON group and CUMS group; $\#p < 0.05$, $\#\#\#p < 0.001$ comparison between the CUMS group and CUMS+MST1 group

4 | DISCUSSION

In the present study, we found that MST1 down-regulation could significantly protect against the impairment of working memory and synaptic plasticity, which were closely associated with regulating the pattern of neural oscillation in depression-like mice. Neural oscillatory analysis showed that not only the theta-band energy was significantly increased, but also both the PLV and the coupling strength from PP to DG were considerably enhanced in the CUMS+MST1 group compared to that in the CUMS group. Moreover, the cross-frequency coupling strength was also significantly increased in the CUMS+MST1 group compared to that in the CUMS group. It suggests that MST1 down-regulation could successfully modulate the neural activities, which were disturbed by CUMS.

4.1 | MST1 knockdown protects against CUMS-induced impairments of working memory synaptic plasticity

Depression is a kind of widespread mental disease, which is manifested as depressed, cognitive impairment, learning & memory ability decline and so on.[20,21] One of our previous studies reported that MST1 down-regulation improved the cognitive impairments induced by stress.[13] In the study, we performed sucrose preference and novel object recognition tests to confirm that exposure to CUMS significantly reduced the sucrose preference and induced the impairment of working memory in mice (Figure 1I–K). However, MST1 knockdown could prevent the appearance of the depression-like behaviors (Figure 1I–K). The data suggest that the abnormality of MST1 activation may play an important role in the pathogenesis of chronic stress-induced mental disorder, and MST1 knockdown effectively improve the working memory deficits in depression-like mice.

Synaptic plasticity is directly related to the strength of neuronal connections and plays a vital role in the structure of the brain network. It is also the basic reason for the change of learning and memory.[22] In this study, we measured LTP and DEP, which were the index representing the intensity changes of synaptic function plasticity. Moreover, the level of PSD95 and SYP proteins related to synapse structure was also measured. SYP is a presynaptic vesicle protein that plays an import role in synaptic vesicle release.[23] The lack of SYP may induce a decrease in synaptic vesicles, which can disturb neurotransmitter release and synaptic network activity.[24] It is reported that several synaptic proteins including PSD95 and SYP play an important role in the regulation of the spine formation and synaptic plasticity.[25] Furthermore, the dendrites of neurons in the hippocampus shrink and the density of dendritic spines decreases in the depression model. Saving dendritic spine loss and synaptic dysfunction, induced by chronic stress, may save depression like behavior.[25] Usually, the slope of the fEPSPs were used for measuring the LTP and DEP.[26,27] In the present study, the amplitudes of the statistical fEPSPs were used for evaluating synaptic plasticity. The analysis shows that LTP and DEP, based on amplitude statistics, has the similar results with our previous study[13](Figure 2A–C). Therefore, our data further suggest that knocking down MST1 can indeed protect against CUMS-induced synaptic plasticity impairments.

4.2 | MST1 knockdown protects against CUMS-induced neural activity disturbance

Synaptic plasticity is generally considered to be a cellular mechanism of learning and memory.[22] Oscillations in neural network temporally links single neurons into assemblies, cooperatively facilitates synaptic plasticity.[11] Generally, theta oscillation is related to the regulation of neural activity and the ability of working memory.[28,29] In addition, the analysis of the power distribution of neural activity, phase synchronization and theta-gamma cross-frequency coupling may well measure neural communication in the context of cognition, learning and memory.[11,16,30] It was also reported that the strength of phase coupling between theta and gamma will change from thalamus to mPFC in depression model rats.[31] In the study, the data showed that power distribution in the CUMS group was evidently disordered, but MST1 knockdown significantly reduced the degree of disturbance (Figure 2D–F, Figure S1A–C). It is worth noting that theta oscillations are also involved in working memory and synaptic plasticity.[32] Meanwhile, the strength of PLV at theta-frequency band was decreased in the CUMS group, but MST1 down-regulation significantly inhibited the reduction (Figure 2G, H), suggesting that it could protect against CUMS-induced synchronization impairment. Furthermore, it reports that the nerve information flow strength of the CUMS group is weakened and is related to synaptic plasticity.[19,33] EMA, as a synchronicity index, measurement showed that it was decreased in CUMS animals, but MST1 knockdown rescued the decrease (Figure 2I, J). To sum up, both PLV and EMA showed that the phase synchronization in the CUMS group was weakened, while MST1 down-regulation significantly improved the synchronization impairment.

Furthermore, cross-frequency coupling, which is a further way to analyze the coupling strength between two different rhythms, has been assessed. In the present study, the PAC-PLV algorithm was applied to analyze theta-gamma coupling, by which the phase of low frequency oscillation adjusts the amplitude of high frequency oscillation could be accurately represented.[34] Gamma rhythm can generally be subdivided into LG and HG, which can differentially encode different network states.[35,36] Indeed, the PAC value of theta-HG was different among the three groups in the hippocampal DG region, and between PP and DG (Figure 2K, L), in which CUMS significantly decreased the PAC but MST1 knockdown considerably alleviated the impairment in mice. It suggests that there is an evidently coupling strength between theta rhythm and the faster spiking gamma rhythm, representing the changes of neural oscillatory patterns and synaptic plasticity. The main source of gamma rhythm is GABAergic interneurons,[37] which can affect the information flow on neural network by controlling the balance of excitability and inhibition.[38]

As we know that the hippocampus DG region plays a key role in cognition and emotion. Moreover, the sub-regions of the hippocampus are closely connected each other, therefore, depression disorders will disturb other brain regions. It has been reported that PLV and EMA between the hippocampal CA1-mPFC are significantly weakened in the animal model of depression, showing that the neural information flow is reduced.[16] In the hippocampus CA1, CA3, and DG, the expression of nerve growth factor was impaired in the rat CUMS model of depression.[39] CUMS led to loss of CA3 neurons in the hippocampus, especially in the right hippocampus.[40] The hippocampus CA3 region is a key brain area of associative memory, and the reduction of neurons disrupts its ability to integrate information. Moreover, as the upstream of CA3, there is a function of pattern separation of input information in the DG sub-region, which directly affects the memory integration and storage capacity of CA3.[41,42] In the study, we found that knockdown of MST1 could protect against the working memory impairment induced by CUMS, implying that knockdown of

MST1 should play a role of protection against memory impairment in other hippocampus regions, such as CA3.

In summary, the data suggest that MST1 knockdown can protect against impairment of working memory via regulating neural activity in depression-like mice. Meanwhile, as a fast and convenient way, neural oscillation analysis is effective in assisting the diagnosis and monitoring of depression.

ACKNOWLEDGMENTS

This work was supported by grants from the National Natural Science Foundation of China (32070988 to TZ) and 111 Project (B08011 to TZ).

CONFLICT OF INTEREST

The authors declare that they have no competing interests.

DATA AVAILABILITY STATEMENT

Data used to support the findings of this study are available from the corresponding author upon request.

ORCID

Tao Zhang https://orcid.org/0000-0002-5743-4657

REFERENCES

1. Zhao S, Yin J, Zhou L, et al. Hippo/MST1 signaling mediates microglial activation following acute cerebral ischemia-reperfusion injury. *Brain Behav Immun*. 2016;55:236-248.
2. Sheng C, Yuanjian F, Shenbin X, Cesar R, Jianmin Z. Mammalian Sterile20-like kinases: Signalings and roles in central nervous system. *Aging Dis*. 2018;9(3):537.
3. Lehtinen MK, Yuan Z, Boag PR, et al. A conserved MST-FOXO signaling pathway mediates oxidative-stress responses and extends life span. *Cell*. 2006;125(5):987-1001.
4. Lee JK, Shin JH, Hwang SG, et al. MST1 functions as a key modulator of neurodegeneration in a mouse model of ALS. *Proc Natl Acad Sci U S A*. 2013;110(29):12066-12071.
5. Yu L, Liu Y, Jin Y, et al. Lentivirus-mediated HDAC3 inhibition attenuates oxidative stress in APPswe/PS1dE9 mice. *J Alzheimers Disease*. 2018;61(4):1411-1424.
6. Quan MN, Zhang N, Wang YY, Zhang T, Yang Z. Possible antidepressant effects and mechanisms of memantine in behaviors and synaptic plasticity of a depression rat model. *Neuroscience*. 2011;182(3):88-97.
7. Aigner M, Sachs G, Bruckmüller E, et al. Cognitive and emotion recognition deficits in obsessive–compulsive disorder. *Psychiatry Res*. 2007;149(1–3):121-128.
8. Wu Y, Mitra R. Prefrontal-hippocampus plasticity reinstated by an enriched environment during stress. *Neurosci Res*. 2020;20:30404.
9. Tort ABL, Komorowski RW, Manns JR, et al. Theta-gamma coupling increases during the learning of item-context associations. *Proc Natl Acad Sci USA*. 2009;106(49):20942-20947.
10. Shang X, Xu B, Li Q, et al. Neural oscillations as a bridge between glutamatergic system and emotional behaviors in simulated microgravity-induced mice. *Behav Brain Res*. 2017;317:286-291.
11. Buzsaki G, Draguhn A. Neuronal oscillations in cortical networks. *Science*. 2004;304(5679):1926-1929.
12. Shang Y, Yan Y, Chen B, Zhang J, Zhang T. Over-expressed MST1 impaired spatial memory via disturbing neural oscillation patterns in mice. *Genes Brain Behav*. 2020;19(6):e12678.
13. Yan Y, Xu X, Chen R, et al. Down-regulation of MST1 in hippocampus protects against stress-induced depression-like behaviours and synaptic plasticity impairments. *Brain Behav Immun*. 2021;94:196-209.
14. Robinson PA, Rennie CJ, Rowe DL, et al. Neurophysical modeling of brain dynamics. *Neuropsychopharmacology*. 2003;28(1):S74-S79.
15. Rosenblum MP. AS detecting direction of coupling in interacting oscillators. *Physreve*. 2001;64(2):045202.
16. Zheng C, Zhang T. Synaptic plasticity-related neural oscillations on hippocampus–prefrontal cortex pathway in depression. *Neuroscience*. 2015;292:170-180.
17. Slavich GM, Irwin MR. From stress to inflammation and major depressive disorder: a social signal transduction theory of depression. *Psychol Bull*. 2014;140(3):774-815.
18. Antoniuk S, Bijata M, Ponimaskin E, Wlodarczyk J. Chronic unpredictable mild stress for modeling depression in rodents: meta-analysis of model reliability. *Neurosci Biobeh Rev*. 2019;99:101-116.
19. Quan M, Zheng C, Zhang N, et al. Impairments of behavior, information flow between thalamus and cortex, and prefrontal cortical synaptic plasticity in an animal model of depression. *Brain Res Bull*. 2011;85(3–4):109-116.
20. Burriss L, Ayers E, Ginsberg J, Powell DA. Learning and memory impairment in PTSD: relationship to depression. *Depress Anxiety*. 2008;25(2):149-157.
21. Perini G, Cotta RM, Sinforiani E, et al. Cognitive impairment in depression: recent advances and novel treatments. *Neuropsychiatr Dis Treat*. 2019;15:1249-1258.
22. Bliss TV, Collingridge GL. A synaptic model of memory: long-term potentiation in the hippocampus. *Nature*. 1993;361(6407):31-39.
23. Yalın OÖ, Edgünlü TG, Çelik SK, et al. Novel SNARE complex polymorphisms associated with multiple sclerosis: Signs of Synaptopathy in multiple sclerosis. *Balkan Med J*. 2019;36(3):174-178.
24. Sasaki MY, Ozawa Y, Kurihara T, et al. Neurodegenerative influence of oxidative stress in the retina of a murine model of diabetes. *Diabetologia*. 2010;53(5):971-979.
25. Hui Q, Li MX, Xu C, et al. Dendritic spines in depression: what we learned from animal models. *Neural Plast*. 2016;2016:1-10.
26. Salazar-Weber NL, Smith JP. Copper inhibits NMDA receptor-independent LTP and modulates the paired-pulse ratio after LTP in mouse hippocampal slices. *Int J Alzheimers Dis*. 2011;2011:864753.
27. McKinney WR, Anders M, Barber SK, et al. Studies in optimal configuration of the LTP. *SPIE Opt Eng Appl*. 2010;7801:780106.
28. Jensen O, Lisman JE. An oscillatory short-term memory buffer model can account for data on the Sternberg task. *J Neurosci*. 1998;18(24):10688-10699.
29. Pfurtscheller G, Neuper C, Pichler-Zalaudek K, Edlinger G, Lopes da Silva FH. Do brain oscillations of different frequencies indicate interaction between cortical areas in humans? *Neurosci Lett*. 2000;286(1):66-68.
30. Kumari E, Shang Y, Cheng Z, Zhang T. U1 snRNA over-expression affects neural oscillations and short-term memory deficits in mice. *Cognitive Neurodynamic*. 2019;13(4):313-323.
31. Zheng C, Zhang T. Alteration of phase–phase coupling between theta and gamma rhythms in a depression-model of rats. *Cognitive Neurodynamic*. 2013;7(2):167-172.
32. O'Neill P-K, Gordon JA, Sigurdsson T. Theta oscillations in the medial prefrontal cortex are modulated by spatial working memory and synchronize with the hippocampus through its ventral subregion. *J Neurosci*. 2013;33(35):14211-14224.
33. Zheng C, Quan M, Yang Z, Zhang T. Directionality index of neural information flow as a measure of synaptic plasticity in chronic unpredictable stress rats. *Neurosci Lett*. 2011;490(1):52-56.
34. Li Q, Zheng CG, Cheng N. Two generalized algorithms measuring phase–amplitude cross-frequency coupling in neuronal oscillations network. *Cognitive Neurodynamic*. 2016;10(3):235-243.
35. Bieri K, Bobbitt K, Colgin L. Slow and fast gamma rhythms coordinate different spatial coding modes in hippocampal place cells. *Neuron*. 2014;82(3):670-681.

36. Schomburg EW, Fernández-Ruiz A, Mizuseki K, et al. Theta phase segregation of input-specific gamma patterns in entorhinal-hippocampal networks. *Neuron*. 2014;84(2):470-485.
37. Gonchar Y, Wang Q, Burkhalter A. Multiple distinct subtypes of GABAergic neurons in mouse visual cortex identified by triple immunostaining. *Front Neuroanatomy*. 2008;2:1–3.
38. Cardin JA, Carlén M, Meletis K, et al. Driving fast-spiking cells induces gamma rhythm and controls sensory responses. *Nature*. 2009; 459(7247):663-667.
39. Song X, Zhang F, Cao L, Wang J. Effect of fluoxetine on nerve growth factor expression in hippocampus CA1,CA3 and DG of rat depression model. *Med J Wuhan Univ*. 2015;36(2):185-188.
40. Hou G, Zhao Y, Yang X, Yuan TF. Autophagy does not lead to the asymmetrical hippocampal injury in chronic stress. *Physiol Behav*. 2015;144:1-6.
41. Lee H, Wang C, Deshmukh S, et al. Neural population evidence of functional heterogeneity along the CA3 transverse Axis: pattern completion versus pattern separation. *Neuron*. 2015;87(5):1093-1105.
42. Yassa MA, Stark Craig CEL. Pattern separation in the hippocampus. *Trends in Neurosciences*. 2011;34(10):515–525.

SUPPORTING INFORMATION

Additional supporting information may be found in the online version of the article at the publisher's website.

How to cite this article: Chen B, Zhang Q, Yan Y, Zhang T. MST1-knockdown protects against impairment of working memory via regulating neural activity in depression-like mice. *Genes, Brain and Behavior*. 2022;21(2):e12782. doi:10.1111/gbb.12782